PHILOSOPHICAL TRANSACTIONS OF THE ROYAL SOCIETY B BIOLOGICAL SCIENCES

Chloride Channels in Toad Skin

E. Hviid Larsen and B. E. Rasmussen

Phil. Trans. R. Soc. Lond. B 1982 **299**, 413-434
doi: 10.1098/rstb.1982.0141

Phil. Trans. R. Soc. Lond. B **299**, 413–434 (1982)
Printed in Great Britain

Chloride channels in toad skin

By E. Hviid Larsen and B. E. Rasmussen

Zoophysiological Laboratorium A, August Krogh Institute, Universitetsparken 13, *DK*-2100 *Copenhagen Ø, Denmark*

A study of the voltage and time dependence of a transepithelial Cl^- current in toad skin (*Bufo bufo*) by the voltage-clamp method leads to the conclusion that potential has a dual role for Cl^- transport. One is to control the permeability of an apical membrane Cl^- pathway, the other is to drive Cl^- ions through this pathway. Experimental analysis of the gating kinetics is rendered difficult owing to a contamination of the gated currents by cellular ion redistribution currents. To obtain insight into the effects of accumulation–depletion currents on voltage clamp currents of epithelial membranes, a mathematical model of the epithelium has been developed for computer analysis. By assuming that the ápical membrane Cl^- permeability is governed by a single gating variable (Hodgkin–Huxley kinetics), the model predicts fairly well steady-state current–voltage curves, the time course of current activations from a closed state, and the dependence of unidirectional fluxes on potential. Other predictions of the model do not agree with experimental findings, and it is suggested that the gating kinetics are governed by rate coefficients that also depend on the holding potential. Evidence is presented that Cl^- transport through open channels does not obey the constant-field equation.

1. Introduction

The present study deals with Cl^- transport through the toad skin. This tissue belongs to the class of NaCl-absorbing epithelia with a low-conductance paracellular shunt. The Cl^- transport therefore takes place predominantly through the surface membranes of epithelial cells. In the skin of anuran amphibians, passive (Koefoed-Johnsen *et al.* 1952*a*) as well as active (Jørgensen *et al.* 1954; Zadunaisky *et al.* 1963) Cl^- transport mechanisms have been found. Both types of mechanism are present in the toad skin. In this paper however, we shall only discuss properties of the passive pathway.

2. Materials and methods

(*a*) *Preparation and experimental procedures*

The abdominal skin of the toad, *Bufo bufo* (L.), isolated in the intermoult period was mounted between Perspex chambers providing space voltage-clamp conditions and minimum edge damage (Koefoed-Johnsen *et al.* 1952*b*). In all of the experiments the inner surface of the skin was exposed to NaCl Ringer solution of the following composition: 112 mM Na^+, 2.4 mM K^+, 1 mM Ca^{2+}, 114 mM Cl^-, 2.4 mM HCO_3^-, pH 8.2, when aerated with atmospheric gas. The outside bathing solution varied and will be referred to as NaCl Ringer, KCl Ringer (Na^+ replaced by K^+) and K-gluconate Ringer (Na^+ and Cl^- replaced by K^+ and gluconate, respectively). In some experiments acetate either as Na^+ or K^+ salt was added to a concentration of 5 mM. Unless otherwise stated the temperature of the bathing solutions was 20–23 °C.

Transepithelial unidirectional Cl^- fluxes were measured with $^{36}Cl^-$ (Danish Atomic Energy Commission, Risø, Denmark) according to Bruus *et al.* (1976).

For voltage clamping conventional circuits with a rise time of transepithelial voltage displacements of 8 μs were used. Computer on-line experiments were performed by using a PDP 11/23

microcomputer (Digital Equipment) for setting command voltage programs and for sampling of transepithelial potentials and clamping currents.

The transepithelial potential is given as the potential in the external bath minus that in the internal bath. Inward currents are taken as positive.

(*b*) *Computer model analysis*

The computer analysis of the mathematical model of the epithelium was performed on a Univac 1100 at the Computing Center of the University of Copenhagen. The computer program was written in the ASCII-FORTRAN language.

(*c*) *Glossary of symbols*

Standard symbols for the Faraday (F), the gas constant (R), and the absolute temperature (T) are used. The symbols for the other quantities used in the text are defined below.

C_j^o, C_j^c, C_j^i	concentration of the ion species, j, in the outer (^{o}), cellular (^{c}), and inner (^{i}) compartments
P_j^o, P_j^{sh}, P_j^i	permeability coefficient of j in the outer (^{o}), paracellular shunt (^{sh}) and inner (^{i}) membranes
$P^o_{Cl^-,\,max}$	fully activated Cl^- permeability in the outer membrane
s	Hodgkin–Huxley gating variable of the outer membrane Cl^- permeability
α, β	potential-dependent rate coefficients of the outer-membrane Cl^- gate.
R^o, R^{sh}, R^i	outer, shunt and inner membrane resistances
G_{slope}	transepithelial slope conductance
V, V_o, V_i	transepithelial, outer-membrane and inner-membrane potential
I_j^o, I_j^{sh}, I_j^i	the current carried by j across the outer, shunt and inner membranes
I^∞	steady-state transepithelial clamping current
I_{Cl^-}	steady-state transepithelial Cl^- current
J_j^o, J_j^{sh}, J_j^i	flux of the ion species j through the outer, shunt and inner membranes
$J^{in}_{Cl^-}$, $J^{out}_{Cl^-}$	transepithelial unidirectional influx (^{in}) and efflux (^{out}) of Cl^-
$J^{i,\,pump}_{Na^+}$, $J^{i,\,pump}_{K^+}$	the Na^+ and K^+ fluxes carried by the inner membrane Na^+/K^+ pump
$J^{i,\,pump}_{Na^+,\,max}$	maximum Na^+ flux of the Na^+/K^+ pump
$K^{i,\,pump}_{Na^+}$	reciprocal of the apparent Na^+ affinity of the Na^+/K^+ pump
Q_j^c	amount of intracellular diffusible ions of species j
Q_x^c	amount of intracellular non-diffusible anions
z_x	the mean valency of intracellular non-diffusible anions
σ_{KCl}	inner-membrane KCl reflexion coefficient
v	cell water volume

3. VOLTAGE-CLAMP EXPERIMENTS WITH TOAD SKIN

(*a*) *Steady-state current–voltage curves*

The toad skin exhibits currents that vary in a nonlinear fashion with the transepithelial potential (Bruus *et al.* 1976; Larsen & Kristensen 1978). This is illustrated in figure 1, in which relations between steady-state current, I^∞, and the transepithelial clamping potential are depicted. With NaCl Ringer bathing both sides, the skin most easily passes current in the outward direction (figure 1*a*). From measurements of unidirectional Cl^- fluxes the Cl^- current can be calculated by $I_{Cl^-} = -F(J^{in}_{Cl^-} - J^{out}_{Cl^-})$, where $J^{in}_{Cl^-}$ and $J^{out}_{Cl^-}$ are the steady-state influx and efflux of Cl^- measured at the same clamping potential. Figure 1*b* shows that the large outward current is carried by an inward-going transport of Cl^- ions, and that I_{Cl^-} becomes close to zero when the skin is clamped to potentials above 0 mV. Replacement of Na^+ by K^+ in the outside bathing solution leads to a significant reduction of the inward current, leaving the large outward currents unaffected (figure 1*c*). These, on the other hand, are reduced by replacing outside

Cl^- by gluconate as illustrated by the broken line in figure 1*c*. Furthermore, with K^+ gluconate Ringer as the outside bathing solution the preparation behaves as a simple ohmic conductor. Taken together, the graphs of figure 1 disclose a rectifying transepithelial Cl^- conductance, the steady-state properties of which do not depend on active Na^+ transport. The rectification is outward-going, i.e. the conductance for outward currents (carried by an inward flux of Cl^-) is larger than the conductance for inward currents. Figure 1*d* shows that the Cl^- conductance increases significantly when going from $V = 0$ mV to $V = -70$ mV, and that the Cl^- conductance becomes constant outside this range of potentials.

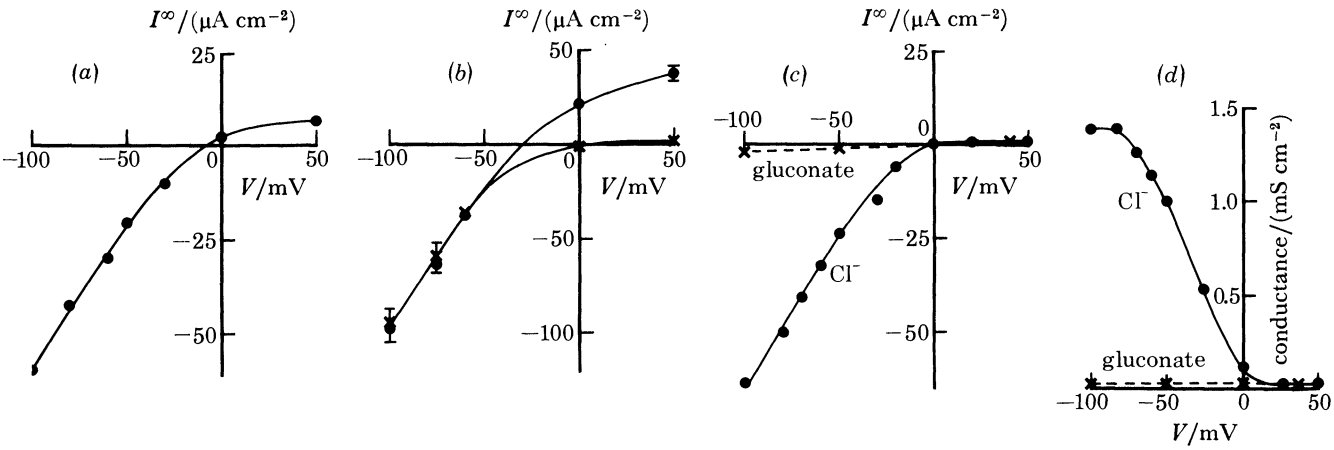

FIGURE 1. (*a*) Steady-state current–voltage (I^∞–V) relation of a toad skin preparation bathed with NaCl Ringer on both sides. The timescale of the experimental analysis is $\frac{1}{2}$–1 h. (*b*) I^∞–V relation in experiments lasting 5–6 h to obtain the current components carried by Cl^- by means of $^{36}Cl^-$ flux measurements. ●, I_{total}; ×, I_{Cl^-}. Mean ± s.e. of five sets of preparations exposed to NaCl Ringer on both sides. (*c*) I^∞–V relation obtained with KCl Ringer (solid curve) or K^+ gluconate Ringer (broken curve) outside. Same skin preparation as in (*a*). Note the close resemblance between the full graph and the I_{Cl^-}–V graph of (*b*). (*d*) Steady-state conductance–voltage curve of the preparation in (*c*). At each clamping potential the conductance was calculated from the current response to a 10 mV potential displacement of 500 ms duration.

Because the Cl^- current is depressed by furosemide, diamox and phloretin, it was concluded that the Cl^- transport is confined to a transcellular route (Kristensen & Larsen 1978).

(*b*) *Mechanism of transport through the* Cl^-*-conductive pathway*

The flux ratio for an ion species moving through a membrane by way of passive diffusion is given by (Ussing 1949, 1978):

$$J^{in}_{Cl^-}/J^{out}_{Cl^-} = ([Cl^-]_o/[Cl^-]_i)\ \exp\ (-FV/RT), \qquad (1)$$

where $[Cl^-]_o$ and $[Cl^-]_i$ are the chemical activities in the outside and inside bathing solutions. With $E_{Cl^-} = (RT/F)\ \ln\ ([Cl^-]_o/[Cl^-]_i)$ we obtain

$$J^{in}_{Cl^-}/J^{out}_{Cl^-} = \exp\ (-F(V-E_{Cl^-})/RT), \qquad (2)$$

where the numerator of the argument is a measure of the externally applied force per mole of Cl^- ions. According to our sign convention this force is positive in an inward direction. In figure 2 is depicted experimental flux ratios on a logarithmic scale against $(V-E_{Cl^-})$. The line represents the theoretical relation for a simple passive pathway. For an outward-directed force (right-hand side of the figure) the experimental flux ratio is up to three orders of magnitude

larger than the theoretical one, indicating that an active or an exchange pathway, or both, govern the Cl^- transport. The participation of an exchange pathway is in agreement with the finding that the flux ratio is close to unity and independent of the outward driving force, whether this is changed by voltage clamping or by reducing the Cl^- activity of the outer bath. The active pathway is disclosed by the flux ratio's being above unity when the Cl^- ions are in electrochemical equilibrium across the skin ($V - E_{Cl^-} = 0$). For an inward-directed force, (2)

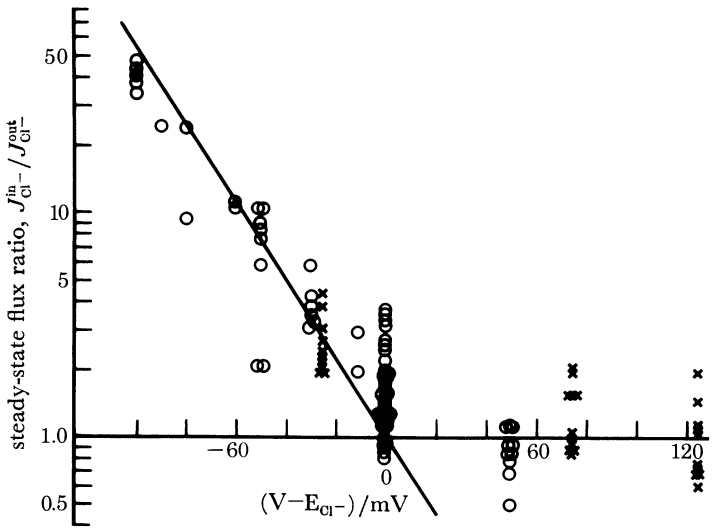

FIGURE 2. Flux ratio analysis of steady-state Cl^- fluxes. Influx and efflux were measured in two skin halves from the same toad. The line is the relation for a simple passive transport in absence of bulk flow of solvent. ○, NaCl Ringer in both inner and outer chamber; × NaCl Ringer inside, 5 mM NaCl Ringer outside. The Cl^- activities of the bathing solutions were calculated according to Bruus *et al.* (1976).

predicts fairly well the experimental flux ratios. From this observation it was suggested that a passive Cl^- permeability varies with transepithelial potential: hyperpolarization of the skin leads to its activation whereas clamping to $V > 0$ mV leads to inactivation (Larsen & Kristensen 1978; Larsen 1982). This hypothesis accounts for the Cl^- current rectification discussed above, and is in agreement with the finding that Cl^- translocation through the activated conductance has a low temperature coefficient (see below).

(*c*) *Time course of current response to stepwise voltage changes*

The results presented above show that a passive transepithelial Cl^- conductance is to be found in a high conductive as well as in a low conductive state, depending on the transepithelial potential. The transition between these states can be studied by following the time response of the current to applied potential steps across the skin. In figure 3*a* is shown a family of current–time curves obtained from a skin exposed to NaCl Ringer on its inner and outer surfaces. Stepping the potential from 50 mV to below 0 mV leads to a rapid initial decrease in currents, which after a significant delay start decreasing towards their new steady levels, illustrating an induced time-dependent conductance increase. Notice that the rate of conductance increase depends on the clamping potential. Returning the potential to 50 mV leads to large inward currents, slowly decaying towards their pre-pulse value of about 6 μA cm^{-2}. Thus the induced conductance changes are fully reversible. Typically, the decay in conductance does not follow a mono-

PHILOSOPHICAL TRANSACTIONS OF THE ROYAL SOCIETY B BIOLOGICAL SCIENCES

exponential time course, as revealed by the 'shoulder' on the current traces especially evident when returning V from clamping potentials below -60 mV. Replacement of outside Na^+ by K^+ does not affect the general picture of current responses with respect to their time course, neither during conductance activation nor during conductance decay after returning V to the holding potential (see figure 3*b*). With K^+ gluconate outside, the slow current responses completely disappear (Larsen & Kristensen 1978; Larsen 1982), in accordance with the linear

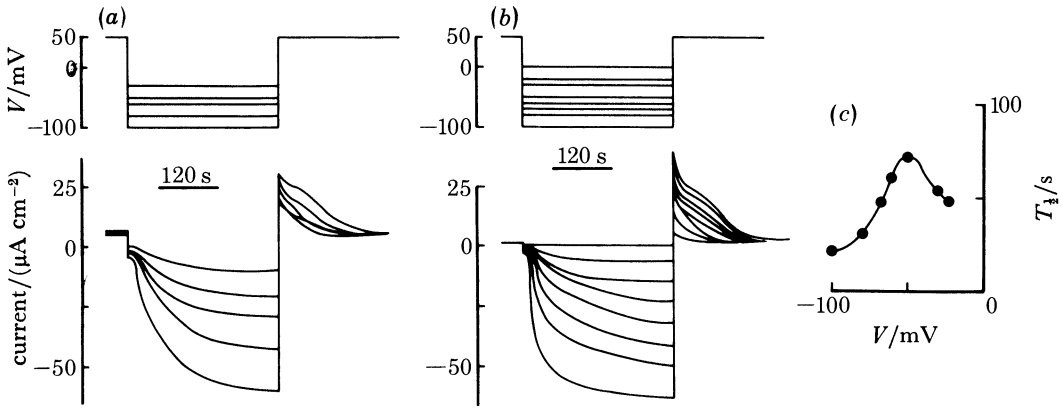

FIGURE 3(*a*). Current response to transepithelial potential pulses of 300 s duration. Potential clamp programme on top. NaCl Ringer inside and outside. (*b*) As in (*a*), but the outside bathing solution is KCl Ringer. (*c*) Potential dependence of the half-time of current activation. The $T_{\frac{1}{2}}$ values are read from the records of (*b*).

current–voltage relation seen in figure 1*c*. The above results will therefore be ascribed to a time-dependent behaviour of an apical membrane conductance specific for Cl^- ions.

The results further illustrate that the macroscopic kinetics of the Cl^- conductance have properties in common with voltage-gated cation channels in excitable membranes (Hodgkin & Huxley 1952) and with conductive pathways induced by pore-forming molecules incorporated into black lipid films (Mueller 1975). This conclusion is substantiated by the fact that the $T_{\frac{1}{2}}$ of current activations depicts a bell-shaped function of clamping potential (see figure 3*c*). If we can assume that the Cl^- pathway is to be found in two configurations only (one non-conductive and one conductive), this finding is compatible with a kinetic scheme governed by rate coefficients for conductance activation with opposite potential dependences. We shall return to this type of model in § 4.

(*d*) *Current-dependent or voltage-dependent* Cl^- *conductance changes?*

General considerations

For a single membrane preparation bathed in well-stirred solutions, results of the type presented above provide evidence that the Cl^- conductance is gated by membrane potential. However, for a multi-membrane system like an epithelium the interpretation of voltage-clamp currents is not that simple. Owing to a low intracellular Cl^- concentration compared with the Cl^- concentration in the bathing solutions, a trivial voltage-dependence of the membrane Cl^- conductances is expected to bring about a significant (outward-going) Goldman rectification (Larsen & Kristensen 1978). Furthermore, slow intracellular Cl^- concentration changes produce current transients even in the absence of gating mechanisms (Larsen *et al.* 1981). The structural complexity of the toad skin preparation therefore imposes considerable difficulties

PHILOSOPHICAL TRANSACTIONS OF THE ROYAL SOCIETY B BIOLOGICAL SCIENCES

in disclosing the nature of time-dependent clamping currents, and more rigorous tests for disclosing voltage-gated processes are required. This type of problem is not unique to epithelial membranes, as preparations of excitable tissues exposed to a restricted non-stirred extracellular compartment present difficulties of similar nature (for a review see Attwell *et al.* 1979). Before proposing any theoretical model it is therefore of significance to obtain further experimental evidence that the transient clamping currents are associated with voltage gating.

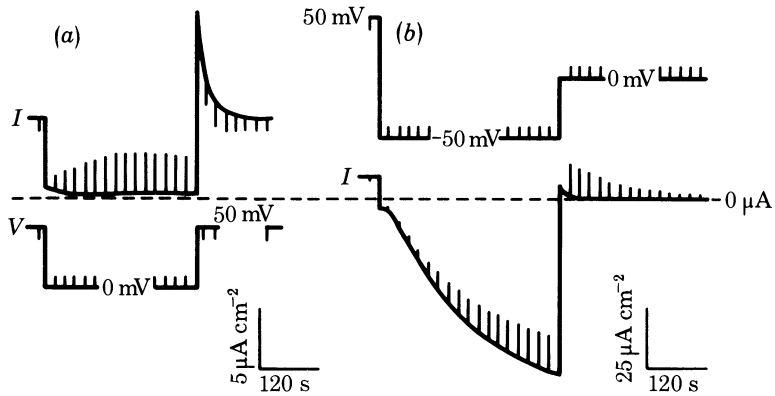

FIGURE 4. Conductance changes in the absence of current flow. NaCl Ringer inside, KCl Ringer outside. The time course of the conductance changes is seen from the clamping current responses to the intermittent 10 mV potential pulses of 500 ms duration. (*a*) Conductance activation initiated by shifting the trans-epithelial potential (V) from 50 to 0 mV. (*b*) Conductance inactivation initiated by a displacement of V from -50 to 0 mV.

Conductance changes at zero current flow

Microelectrode studies by Helman & Fisher (1977) and by Nagel (1977) have shown that in the short-circuited amphibian skin exposed to KCl Ringer outside the intracellular potential is about 100 mV below that of the external solutions, and that the ratio of the outer membrane resistance to the transcellular resistance is above 0.9. Thus a displacement of the transepithelial potential from $V > 0$ mV to, say, $V = -100$ mV leads to a significant (instantaneous) depolarization of the outer membrane and a smaller hyperpolarization of the inner membrane. Provided that the outer membrane is permeable to Cl^- and the inner membrane has a K^+ permeability of the same magnitude or larger than its Cl^- permeability, this will start a cellular accumulation of Cl^- supplied from the outer bath, and of K^+ supplied from the inner bath. Thus, an outward-going transepithelial current flows, carried by Cl^- through the outer membrane and by K^+ through the inner membrane. In the absence of gating mechanisms the increase in membrane conductances is associated with and decays with the transient transepithelial current (Larsen *et al.* 1981).

In an attempt to test this possibility, we studied the time course of the transepithelial conductance under conditions of zero membrane current in which intracellular ion accumulation or depletion do not occur. In figure 4*a* the potential is displaced from 50 mV to 0 mV and back. Notice the large instantaneous 'off' response of the clamping current following the return of V to 50 mV. This illustrates that a significant conductance increase has taken place during voltage clamping to 0 mV, despite the current's being very near to zero. The conductance time course is shown by the current responses to the intermittent 10 mV pulses. In figure 4*b*, the Cl^-

conductance was activated by voltage clamping to −50 mV, and subsequently the potential was pulsed back to 0 mV. Here a significant conductance decrease takes place under conditions of zero membrane current. Thus neither conductance activation nor conductance decay depends on current flowing through the epithelium. This shows that potential and not current flow controls the time-dependent properties of the Cl^- conductance.

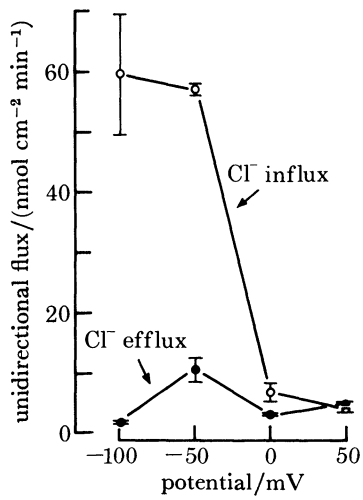

FIGURE 5. Potential dependence of the steady-state unidirectional Cl^- fluxes. NaCl Ringer on both sides. Each set of preparations was measured at 0 mV (n = 18) and at one of the following potentials: −100 mV (n = 5), −50 mV (n = 7), and 50 mV (n = 6) (Means ± s.e.).

Potential dependence of unidirectional fluxes

The potential dependence of steady-state unidirectional Cl^- fluxes has been published previously (Bruus *et al.* 1976). We include here new measurements and present them in figure 5, together with previous measurements. The first important observation is that neither Cl^- influx nor Cl^- efflux change much by stepping the potential from 0 to 50 mV. These fluxes are therefore probably carried by a 1:1 Cl^- exchange pathway as discussed above. Next, the Cl^- influx increases with hyperpolarization, as expected for a negatively charged ion moving through the membrane driven by the electrical potential difference. Likewise the Cl^- efflux is significantly smaller at −100 mV than at 0 mV. However, there is an increase in Cl^- efflux when V is shifted from 0 to −50 mV, despite the fact that this potential change is also expected to impede backflux of Cl^- ions moving along a passive pathway. This shows that the freedom with which the Cl^- ions move through the skin undergoes a significant change in this potential range, and it supports the hypothesis that the potential, besides providing the driving force for Cl^- transport, also controls the Cl^- permeability.

Experiments at low temperature

In voltage-clamped excitable membranes the rate of conductance activation has a much stronger temperature dependence than the fully activated conductance (Hodgkin *et al.* 1952; Moore 1958; Frankenheuser & Moore 1963; Tsien & Noble 1969). This applies to toad skin as well. For example, figure 6*a* depicts the time courses of Cl^- conductance activation at 22 and

PHILOSOPHICAL TRANSACTIONS OF THE ROYAL SOCIETY B BIOLOGICAL SCIENCES

14 °C initiated by pulsing the transepithelial potential from 40 to −75 mV. In figure 6*b* the two graphs are superimposed by scaling the conductance axis of the 22 °C graph by a factor of 1/1.13 and its time axis by 1.60. This shows that the rate at which the conductance changes with time is more sensitive to a fall in temperature than the conductance itself. The time constant of conductance activation may be expressed by the half-time ($T_{\frac{1}{2}}$) of the conductance shift from the inactivated to the fully activated state. In the temperature interval between 8 and

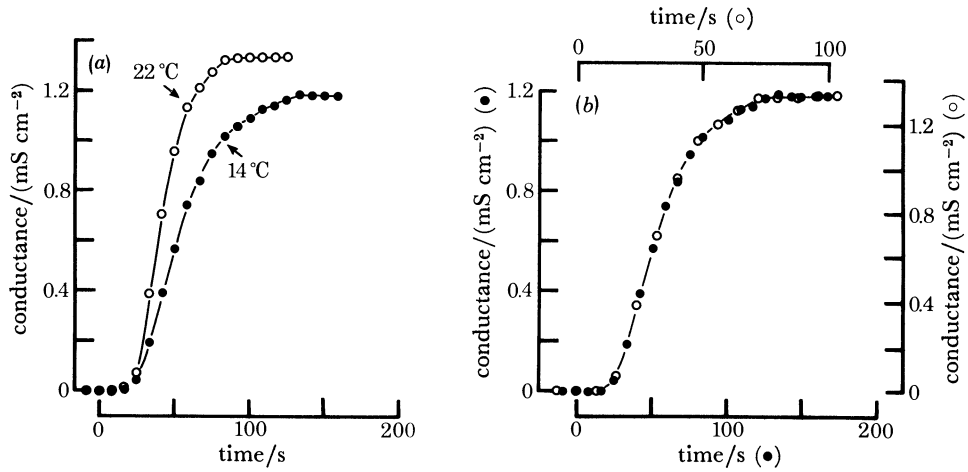

FIGURE 6. (*a*) Effect of changing the temperature of the bathing solutions on conductance activation in toad skin exposed to NaCl Ringer inside and KCl Ringer outside. At zero time the transepithelial potential was displaced from 40 to −75 mV. (*b*) The two graphs of (*a*) are superimposed by scaling the time axis of the 22 °C graph by a factor of 1.60 and its conductance axis by a factor of 0.885.

23 °C, $1/T_{\frac{1}{2}}$ yields a straight line in an Arrhenius plot, as also occurs for the fully activated conductance (Larsen *et al.* 1981). In this temperature interval the temperature coefficient of conductance activation varied for nine preparations between 1.8 and 2.3 whereas the temperature coefficient of the fully activated conductance varied between 1.1 and 1.5 (Willumsen & Larsen 1981). A closer quantitative analysis of the effect of temperature on conductance activation presupposes more detailed knowledge about the kinetics of the activation process than we have at present. But the above results justify that we should, in what follows, treat ion translocation and conductance activation as separate processes.

4. Computer analysis of the Koefoed-Johnsen–Ussing model

(*a*) *Outline of the mathematical model and computational strategy*

The mathematical model of the epithelium is based on the two-membrane model of Koefoed-Johnsen & Ussing (1958) supplied with a paracellular shunt (Ussing & Windhager 1964) (see figure 7).

Cell volume adjustments are allowed for by assuming the existence of a fixed amount, Q_x^c, of impermeable intracellular anions,

$$v = Q_x^c / C_x^c, \tag{3}$$

with a concentration C_x^c governed by the assumption of isosmolarity in the serosal and the cellular compartments,

$$C^i_{Na^+} + (2\sigma_{KCl} - 1)\, C^i_{K^+} + C^i_{Cl^-} = C^c_{Na^+} + C^c_{K^+} + (2\sigma_{KCl} - 1)\, C^c_{Cl^-} + C^c_x. \tag{4}$$

PHILOSOPHICAL TRANSACTIONS OF THE ROYAL SOCIETY B BIOLOGICAL SCIENCES

Since Cl^- and K^+ are expected to pass freely through the inner membrane, a KCl reflexion coefficient σ_{KCl} has been included.

The turnover of the Na^+/K^+ pump in the inner membrane is described by the equations

$$J^{i,\,pump}_{Na^+} = J^{i,\,pump}_{Na^+,\,max}\,\{C^c_{Na^+}/(C^c_{Na^+} + K^{i,\,pump}_{Na^+})\}^3 \tag{5}$$

and

$$J^{i,\,pump}_{K^+} = -\tfrac{2}{3}\,J^{i,\,pump}_{Na^+}, \tag{6}$$

showing saturation for $C^c_{Na^+} \gg K^{i,\,pump}_{Na^+}$.

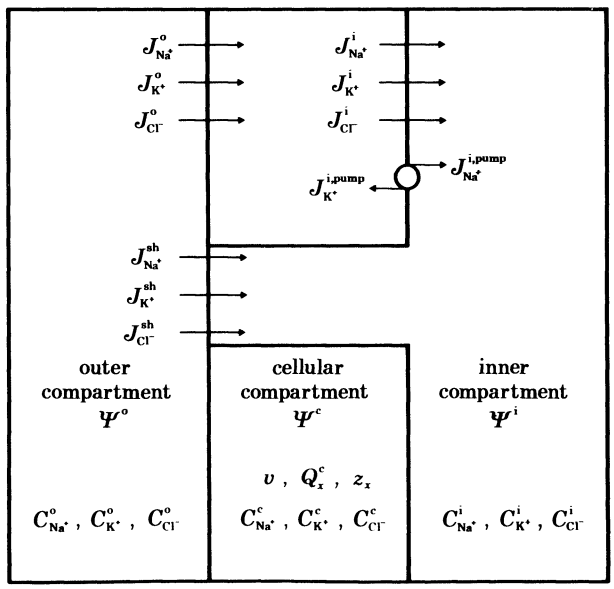

FIGURE 7. Diagram of the three-compartment model analysed in the present paper. The inner and outer compartments are assumed infinitely large. Ψ^o, Ψ^c and Ψ^i are the electrical potentials of the outer, cellular and inner compartments, respectively. For definition of the symbolic representation see §2*c*.

For each permeable ionic species j we assume that the passive flux through the shunt, the outer and the inner membrane, respectively, is described by an integrated Nernst–Planck equation,

$$J^{sh,\,passive}_j = P^{sh}_j \frac{z_j FV/RT}{1-\exp\,(z_j FV/RT)}\{C^i_j - C^o_j \exp\,(z_j FV/RT)\}, \tag{7a}$$

$$J^{o,\,passive}_j = P^o_j \frac{z_j FV_o/RT}{1-\exp\,(z_j FV_o/RT)}\{C^c_j - C^o_j \exp\,(z_j FV_o/RT)\}, \tag{7b}$$

$$J^{i,\,passive}_j = P^i_j \frac{z_j F(V-V_o)/RT}{1-\exp\,(z_j F(V-V_o)/RT)}[C^i_j - C^c_j \exp\,\{z_j F(V-V_o)/RT\}], \tag{7c}$$

where $V = \Psi^o - \Psi^i$, $V_o = \Psi^o - \Psi^c$ and $j = Na^+$, K^+ or Cl^-.

All permeabilities except $P^o_{Cl^-}$ are assumed to be constant (i.e. independent of voltage and concentration). $P^o_{Cl^-}$ is governed by the following Hodgkin–Huxley-like equations:

$$P^o_{Cl^-} = P^o_{Cl^-,\,max}\,s^6, \tag{8}$$

$$ds/dt = \alpha(1-s) - \beta s, \tag{9}$$

$$\alpha = 0.0014\,(V_o - 85)/[\exp\{\tfrac{1}{12}(V_o - 85)\} - 1], \tag{10}$$

$$\beta = 0.06/[\exp\{-\tfrac{1}{3}(V_o - 80)\} + 1]. \tag{11}$$

Mass conservation in the cellular compartment is expressed by the continuity equations

$$dQ_j^c/dt = J_j^o - J_j^i, \tag{12}$$

$$C_j^c = Q_j^c/v, \tag{13}$$

where J_j^o and J_j^i are the sums of passive and pump fluxes of ionic species j(= Na^+, K^+ or Cl^-) through the outer and inner membrane, respectively. Finally, we introduce a quantity d_c proportional to the net charge density in the cell,

$$d_c = C^c_{Na^+} + C^c_{K^+} - C^c_{Cl^-} + z_x C^c_x, \tag{14}$$

and ask that any physical solution to the above set of equations must fulfil the electroneutrality condition, i.e. the net charge density must equal zero.

This set of equations constitutes a well posed mathematical problem, as is most easily seen in the steady-state voltage-clamp situation, where

$$ds/dt = 0 \Rightarrow s = \alpha/(\alpha+\beta); \tag{15}$$

$$dQ_j^c/dt = 0 \Rightarrow J_j^o = J_j^i; \quad j = Na^+, K^+ \text{ or } Cl^-. \tag{16}$$

Taking outer membrane potential V_0 and cellular concentrations $C^c_{Na^+}$, $C^c_{K^+}$, $C^c_{Cl^-}$ and C^c_x as the primary unknowns, (10), (11), (15) and (8) determine $P^o_{Cl^-}$ (5), (6) and (7) determine the ionic fluxes, and volume is determined from (3). In turn, the five primary unknowns are determined from the three continuity equations, (16), the isosmolarity assumption, (4), and the electroneutrality condition, (14).

The actual line of computations is as follows. An initial value of V_0 is guessed, based on knowledge of the transcellular resistance divider ratio; s and $P^o_{Cl^-}$ are computed, and (16) are solved for $C^c_{Na^+}$, $C^c_{K^+}$ and $C^c_{Cl^-}$. This can be done explicitly for $C^c_{Cl^-}$. Owing to the nonlinear dependence of pump fluxes on $C^c_{Na^+}$, one has to apply an iterative scheme for $C^c_{Na^+}$ and $C^c_{K^+}$. Then C^c_x is determined from (4) and the net charge density, d_c, is computed from (14).

This sequence of computations is repeated, using the secant method to correct V_0, until d_c equals zero. Then volume, net fluxes, unidirectional fluxes, currents, conductances, etc. are computed.

Unidirectional isotope fluxes are computed for a multicompartment system (Ussing & Zerahn 1951). Ionic conductances through the single membranes are computed on the basis electrodiffusion theory (Sten-Knudsen 1978). The composite membrane system is also described by a slope conductance defined as the ratio

$$G_{slope} = \Delta I/\Delta V, \tag{17}$$

where ΔI is the instantaneous change in total membrane current after a sudden displacement, ΔV, of the transepithelial potential 5 mV up and down with respect to the present V.

To handle the steady-state current-clamp situation one more level of iteration is used. Initially, the total membrane current is computed as above for $V = 0$. V is then stepped up or down by using the secant method until the computed current and the clamping current are equal.

To solve the equations in the non-steady-state voltage-clamp situation the following procedure is used. An instantaneous step of potential from a holding value to a clamp value initially leaves $P^o_{Cl^-}$ and the cell concentrations unchanged at their steady-state values at the holding state. The passive fluxes $J_j^{m,\,passive}$, however, are changed instantaneously and, as a consequence

PHILOSOPHICAL TRANSACTIONS OF THE ROYAL SOCIETY B BIOLOGICAL SCIENCES

V_0 is also changed. The instantaneous V_0 is found from the requirement that the electrical current across inner and outer membranes must be equal:

$$J^{o}_{Na^+} + J^{o}_{K^+} - J^{o}_{Cl^-} = J^{i}_{Na^+} + J^{i}_{K^+} - J^{i}_{Cl^-}. \quad (18)$$

V_0 is determined iteratively by using the secant method, and instantaneous values of fluxes, currents, etc., are computed. This procedure defines an instantaneous non-steady state. Also the rate constants α and β are changed instantaneously, their new values being determined from the new V_0 and (10) and (11). Since initial values for s and Q^c_j are available, we are now ready to solve the set of coupled differential equations (9) and (12), yielding s and Q^c_j as functions of time. This is done by using a fourth-order Runge–Kutta integration procedure. After each integration step new concentrations are determined from (13) and (4), and the new volume from (3). New fluxes are determined from (5), (6) and (7), and a new V_0 is determined from (18) as described above. This procedure is continued until transient values for s and C^c_j have reached their final steady-state values, which are computed before the integration procedure is initiated. In the actual computations the time increment is adjusted automatically to obtain good computing accuracy and to avoid excessive computing time and cost.

The computations in the non-steady-state current-clamp situation are slightly more complicated. After each integration step, a new V_0 cannot be determined from (18) as in the voltage-clamp mode, since now V also varies with time. The requirement that the total clamping current must equal the sum of the shunt and the cellular current provides the extra condition needed to set up an iterative scheme whereby V and V_0 are simultaneously corrected towards their physical values.

(*b*) *The short-circuited model*

In the remaining part of this section we discuss the electrical behaviour of the model whose properties are defined by the above equations. With the notable exception of the dynamic Cl^- permeability, mathematical treatments of the two-membrane model are available in the literature (Lindemann 1977*a*, *b*; Lew *et al.* 1979). As pointed out in those papers, the strength of this approach lies in its power to analyse the behaviour of a model that is too complicated to be understood intuitively. Its weakness comes from the fact that the input parameters are not all available from direct measurements. Thus the first step is to choose values of unknown input parameters that lead to a reproduction of intracellular concentrations, membrane potentials and resistances of the living tissue obtained within a certain experimental régime. Next the model is subject to experimental tests to see how accurately it represents the epithelial membrane outside this régime. This part of the analysis may provide useful information about the validity of assumptions regarding the individual membrane pathways. As suggested by Lew *et al.* (1979), a step-by-step analysis and correction of the model provides a rigorous way of developing quantitative models of such a complicated experimental system as epithelial membranes.

Because the amphibian skin has been studied more intensively in the short-circuit condition than in any other condition, this is the reference experimental condition for choice of the standard input parameters given in table 1. The values of inner-membrane pump constants (Larsen *et al.* 1979; Nielsen 1982), the outer membrane's permeability to Na^+ (Fuchs *et al.* 1977), and the permeabilities of the paracellular shunt (Bruus *et al.* 1976) are in agreement with experimental findings in the studies listed above. The outer membrane's permeability to K^+ and the inner membrane's permeabilities to K^+ and Cl^- are not as well characterized experimentally, and other values of these parameters may be used. For clarity we use only this set of

PHILOSOPHICAL TRANSACTIONS OF THE ROYAL SOCIETY B BIOLOGICAL SCIENCES

parameters in the following presentation, but a large number of other combinations have been tested to ensure that the points to be discussed are not dependent on this particular choice of values.

With this set of standard input parameters we obtain a short-circuit current of 19.9 μA cm^{-2} and an open-circuit potential of −35.6 mV, which compare well with measured values (figure 1*b*). Likewise, the computed intracellular concentrations of Na^+ and K^+, as well as the membrane potentials and their resistances, are within the range recently measured in amphibian skin (see table 2). Notice, however, that the computed intracellular Cl^- concentration is significantly smaller than that of the granulosum cells of the frog skin. This pertinent shortcoming of the model was discussed by Lew *et al.* (1979), and we shall discuss its implications in §5*a*.

TABLE 1. STANDARD VALUES OF INPUT PARAMETERS USED FOR THE COMPUTATIONS PRESENTED IN THIS PAPER

parameter	unit	value
$C^{o}_{Na^+}$, $C^{i}_{Na^+}$	mM	112
$C^{o}_{K^+}$, $C^{i}_{K^+}$	mM	2.4
$C^{o}_{Cl^-}$, $C^{i}_{Cl^-}$	mM	114.4
$P^{o}_{Na^+}$, $P^{o}_{K^+}$, $P^{o}_{Cl^-,\,max}$	cm s^{-1}	5×10^{-7}, 10^{-7}, 10^{-5}
$P^{i}_{Na^+}$, $P^{i}_{K^+}$, $P^{i}_{Cl^-}$	cm s^{-1}	10^{-8}, 2.5×10^{-5}, 1.2×10^{-5}
$P^{sh}_{Na^+}$, $P^{sh}_{K^+}$, $P^{sh}_{Cl^-}$	cm s^{-1}	1.7×10^{-8}, 2.5×10^{-8}, 10^{-8}
$J^{i,\,pump}_{Na^+,\,max}$	mol cm^{-2} s^{-1}	6×10^{-10}
$K^{i,\,pump}_{Na^+}$	mM	3.4
σ_{KCl}	—	0.95
Q^{c}_{x}	mol cm^{-2}	2.5×10^{-8}
z_x	equivalents mol^{-1}	−2
T	K	293

TABLE 2. INTRACELLULAR CONCENTRATIONS, MEMBRANE POTENTIALS, AND RESISTANCES OF THE MODEL COMPARED WITH MEASURED VALUES IN AMPHIBIAN SKIN

(Superscripts indicate whether the values are given for short-circuit (^{sc}) or open-circuit (^{open}) conditions. V^{sc}_{o} is the potential in the outer solution minus that in the cell. V^{open}_{i} is the potential in the cell minus that in the inside solution.)

	model	skin
$C^{c,\,sc}_{Na^+}$	8.2 mM	7 ± 4.5 mmol kg^{-1} wet mass*, 14 ± 3 mM†, 7.9 mM‡
$C^{c,\,sc}_{K^+}$	143 mM	112 ± 12 mmol kg^{-1} wet mass*, 132 ± 10 mM†
$C^{c,\,sc}_{Cl^-}$	3.1 mM	36 ± 5.0 mmol kg^{-1} wet mass*, 18 ± 3 mM†
V^{sc}_{o}	91 mV	73 ± 2.3§, 98 ± 4.1‖, 104 ± 2.6¶, 98** mV
V^{open}_{i}	−95 mV	−108 ± 1.6 mV§
R^{sc}_{o}	7.6 kΩ cm^2	4.7 ± 1.1¶, 7.9** kΩ cm^2
R^{sc}_{i}	0.6 kΩ cm^2	0.5 ± 0.12¶, 1.9** kΩ cm^2

* *Rana temporaria*. Electron microprobe analysis. The mean dry mass of the tissues was 25.4 ± 2.3 g per 100 g (Rick *et al.* 1978).
† *R. pipiens*. Activities measured with ion selective microelectrodes (Nagel *et al.* 1981).
‡ *R. temporaria*. Concentration in the cellular Na^+ transport pool exchanging with Na^+ of the outside bath (Nielsen 1982).
§ *R. temporaria* and *R. esculenta* (Nagel 1976).
‖ *R. pipiens* (Helman & Fisher 1977).
¶ *R. pipiens* (Helman *et al.* 1979).
** *Bufo marinus* (Nagel & Crabbé 1980).

PHILOSOPHICAL TRANSACTIONS OF THE ROYAL SOCIETY B BIOLOGICAL SCIENCES

(*c*) Cl^- *current rectification*

In our previous mathematical analysis of the two-membrane model we assumed that the outer membrane's permeability to Cl^- was independent of membrane potential (Larsen & Kristensen 1978; Larsen *et al.* 1981). An interesting outcome of this analysis was the fact that a Goldman rectification produces steady-state current–voltage curves resembling those of the toad skin. For the following reasons this simple version of the model has had to be discarded. (i) The large outward currents for $V < -50$ mV presuppose such a large $P^o_{Cl^-}$ that the Cl^- currents for $V > 0$ mV also contribute significantly to the total clamping current. Isotope flux measurements have shown that the Cl^- current is not significantly different from zero for $V = 50$ mV. (ii) Pure accumulation–depletion currents decay almost mono-exponentially, i.e. without the initial delay of clamping currents in toad skin. (iii) After the displacement of V from 0 mV to large negative values, the time constant of the transient currents increases with the amplitude of the potential pulse. This is in contrast to experimental findings. The result of this analysis therefore justifies the extending of the computer model with a potential–dependent Cl^- permeability.

Our starting point is a Hodgkin–Huxley type theory (Hodgkin & Huxley 1952) expressed mathematically by (8)–(11). The assumptions are that the Cl^- channel is to be found in only two configurations (open and closed), and that the rate coefficients governing transitions among these are potential-dependent. Tentatively, the delay in Cl^- current activation is accounted for by raising the gating variable to the power of six (equation (8)). Equations (10) and (11) defining the potential dependence of the rate coefficients, were chosen to fit certain aspects of the experimental data, namely the steady-state current–voltage curve and the timescale of clamping currents associated with a permeability change from the closed to the fully activated state.

With the above equations, the computed steady-state current–voltage curve is nonlinear with large transcellular Cl^- components for $V < -50$ mV (see figure 8*a*). According to the model the outer membrane's permeability to Cl^- is very nearly zero for $V > 0$ mV. Thus the inward currents in this region are carried by the active Na^+ pathway, in agreement with experimental findings (see Bruus *et al.* (1976) and figure 1*b*). For $V = 50$ mV, $C^c_{Na^+} = 13.4$ mM, $C^c_{K^+} = 138$ mM, and $C^c_{Cl^-} = 3.9$ mM. For $V = -100$ mV the corresponding values are 2.9, 144 and 20.9 mM, respectively. Probably, these concentration changes, together with the concomitant increase in cell water volume from 339 to 397 nl cm^{-2}, are tolerated by a living tissue.

The time course of clamping currents of the model with NaCl Ringer in the outside compartment is shown in figure 8*b*. Owing to changes of the amount of intracellular ions with potential, these clamping currents are not pure gated currents, but they also contain components associated with the ion redistributions. Another complication comes from the fact that the outer membrane potential changes, despite the transepithelial potential's being kept constant. The time constant of the permeability activation therefore varies with time. This is an important notion, because it implies that the kinetics of the clamping currents may not give the desired information about the gating reaction. For example, after a displacement of V from 50 to -100 mV the instantaneous value for the outer membrane potential (V_o) is 0 mV. In the course of the first 20 s, V_o increases towards 16 mV, whereafter V_o slowly returns to 1 mV (its new steady-state value). The corresponding values for the time constant, $\tau(= 1/(\alpha+\beta))$ are 8.4, 10 and 8.5 s, respectively. Replacement of Na^+ by K^+ in the outer compartment takes away the current carried by the active Na^+ pathway (figure 8*c*). In this case, the intracellular

PHILOSOPHICAL TRANSACTIONS OF THE ROYAL SOCIETY B BIOLOGICAL SCIENCES

Na^+ concentration is below 1 mM and independent of V. However, during activation at $V = -100$ mV, the intracellular Cl^- concentration, as well as V_0, change as much as before. Since Cl^- and K^+ are taken up from the external and internal compartment, respectively, these ion accumulations are associated with a transcellular current superimposed on the gated current. One might suggest that separation of these current components is possible by monitoring the time-dependence of intracellular concentrations by ion-selective microelectrodes. Our

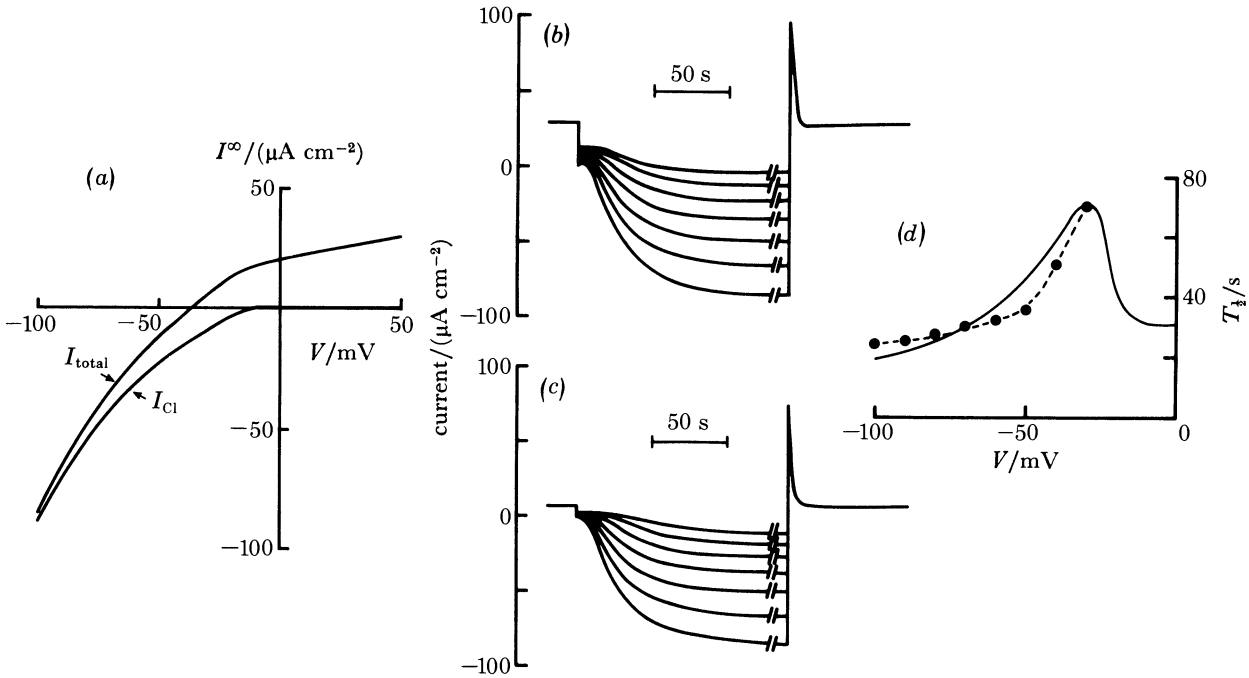

FIGURE 8. Model analysis based on the standard input parameter set given in table 1. (*a*) Steady-state total current–voltage curve of the model with the Cl^- current–voltage relation included. (*b*) Voltage-clamp currents of the model. Holding potential 50 mV, clamping potential from −100 to −40 mV in steps of 10 mV. (*c*) Voltage-clamp currents of the model after replacement of Na^+ by K^+ in the outer compartment. Potential pulse programme as in (*b*). (*d*) Solid line, potential dependence of the half-time of Cl^- permeability activation. At the holding potential ($V = 50$ mV), $P^o_{Cl^-} = 0$. The half times can therefore be calculated from $T_{\frac{1}{2}} = \ln\{1/(1-\sqrt[6]{0.5})\}/(\alpha+\beta)$, where α and β are the steady-state rate coefficients at the clamping potentials. ●, $T_{\frac{1}{2}}$ values from the current activations in (*c*).

analysis indicates that it is not that simple. The accumulation current depends on the amount of KCl taken up by the cellular compartment. Our calculations show that in the course of permeability activation the cell water volume is expected to increase. The water uptake dilutes the intracellular constituents to such an extent that $C^c_{K^+}$ decreases with time, despite the fact that a net uptake of K^+ takes place. Thus the ion redistribution current cannot be determined experimentally unless the time-dependences of intracellular ion concentrations and cell volume are measured simultaneously. So even if a successful clamping of the outer membrane potential is achieved, there is no easy way to obtain the pure gated currents of this system.

On the other hand, our calculations also indicate that with KCl in the outer compartment the time course of clamping currents is governed predominantly by the gating changes. This is illustrated in figure 8*d*. The solid line depicts the potential dependence of the steady-state time constant of the permeability activation. The symbols show the potential dependence of

PHILOSOPHICAL TRANSACTIONS OF THE ROYAL SOCIETY B BIOLOGICAL SCIENCES

the time constant of the clamping currents (read from the graphs of figure 8*c*). The agreement is not too bad. If the three-compartment model is a good description, it therefore seems that useful information of the gating reaction can be obtained by an analysis of the time course of transepithelial clamping currents.

The potential dependence of the steady-state unidirectional fluxes of the model are shown in figure 9. The large differences between fluxes of the model and the toad skin for $V = 0$ mV (compare with figure 5) are assumed to be due to a significant contribution from an exchange

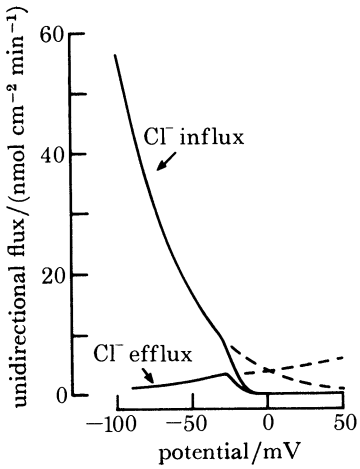

FIGURE 9. Dependence of unidirectional Cl^- fluxes of the model on the transepithelial potential. Solid lines show the relation for the case where $P^o_{Cl^-}$ depends on the outer membrane potential according to the kinetic scheme given in the text. The broken right-hand continuations of the graphs show the potential dependence of the fluxes for the case where $P^o_{Cl^-}$ is not inactivated ($P^o_{Cl^-} = 10^{-5}$ cm s^{-1} throughout).

pathway in the skin. The evidence for this hypothesis has been discussed above. Because the exchange pathway is not included in the model, it follows that the Cl^- fluxes of the model for $V = 0$ mV are governed by the passive conductors. Of more interest is the fact that the efflux of Cl^- is predicted to increase after a displacement of V from 0 to -50 mV, as observed in the toad skin (figure 5). This response cannot be accounted for in a constant-permeability régime as is illustrated by the broken lines in figure 9.

In figure 10 is depicted the potential dependence of the steady-state (slope) conductance of the model. Although the outer membrane's permeability to Cl^- saturates for $V < -50$ mV (broken line), the conductance continues to increase with decreasing transepithelial potential. This is in contrast to the potential variation of the conductance in the skin, which typically saturates like the permeability (compare with figure 1*d*). The rectification of the model in excess of that predicted by the permeability activation depends on the rectifying properties of open channels. Thus it is indicated that the constant-field theory is inadequate for describing the kinetics of Cl^- ion translocation through open channels. Alternatively it may be assumed that a transport system not included in the model raises the intracellular Cl^- concentration of the skin above its passive distribution. This would lead to less constant-field rectification in the fully activated pathway.

(*d*) *The gating kinetics*

It has been noted (Willumsen & Larsen 1981; Larsen 1982) that in some skins the time course of current activation and decay seemed inconsistent with a simple Hodgkin–Huxley kinetic

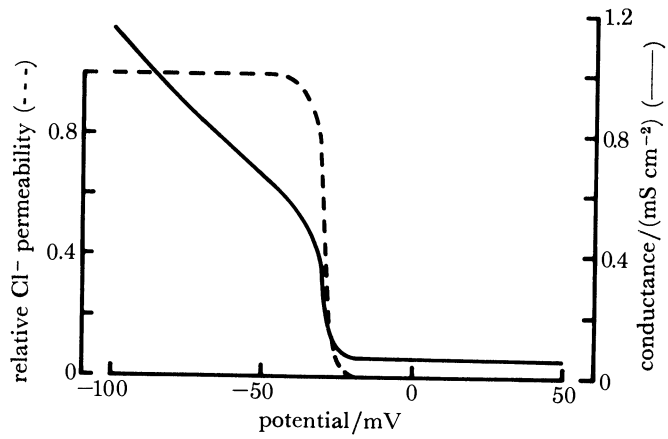

FIGURE 10. Transepithelial potential dependence of the steady-state slope conductance of the model (solid line). These computations simulate the type of experiment illustrated in figure 1*d*. The steady-state outer membrane Cl^- permeability (given as $P^o_{Cl^-}/P^o_{Cl^-,max}$) is shown by the broken line. Note that the permeability saturates for $V < -50$ mV, in contrast to the conductance.

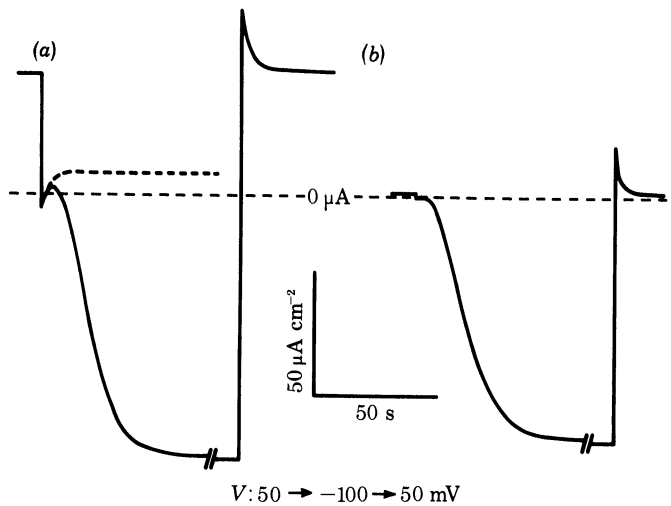

FIGURE 11 (*a*). Computer prediction of the cation redistribution current of the model. A small cellular compartment of the model is assumed. The positive-going current transient preceding the current activation is associated with the decay of cellular Na^+ depletion through the outer membrane, and K^+ accumulation through the inner membrane. To accentuate this current component $P^o_{Na^+}$ and $P^i_{K^+}$ have also been changed, but kept within the physiologically resonable range. To illustrate the time course of the cation redistribution component, the broken line shows the clamping current response of the model for the case where $P^o_{Cl^-}$ stays near zero. Input parameters are as given in table 1, but $P^o_{Na^+} = 10^{-6}$ cm s^{-1}, $P^i_{K^+} = 2 \times 10^{-6}$ cm s^{-1}, and $Q^c_x = 10^{-8}$ mol cm^{-2}. (*b*) Clamping current response of the model after replacement of Na^+ in the outer compartment by K^+; otherwise, the same input parameters of the model are used as in (*a*).

scheme. Thus activation was preceded by a decrease in conductance instead of a delay. Furthermore, when pulsing V back to the holding potential the current decayed with a pronounced hump superimposed on the expected exponential-like time course. This latter response is also typical of the current traces shown in figure 3*a*, *b*.

To begin with, we may ask whether these deviations from the expected current–time curves are caused by accumulation–depletion currents superimposed on the gated current. After a

PHILOSOPHICAL TRANSACTIONS OF THE ROYAL SOCIETY B BIOLOGICAL SCIENCES

change in V from 50 mV to large negative values, the driving forces acting upon the Na^+ ions crossing the outer membrane, and upon the K^+ ions crossing the inner membrane, both change sign. The resulting cation movements are associated with a transepithelial outward-going current component that decays with time as the new steady-state intracellular concentrations of Na^+ and K^+ are approached. If we assume a smaller cell volume than in the above calculations this decay of the outward-going cation current of the model is clearly seen, as it now precedes the gated current (figure 11*a*). The type of response of clamping current depicted in

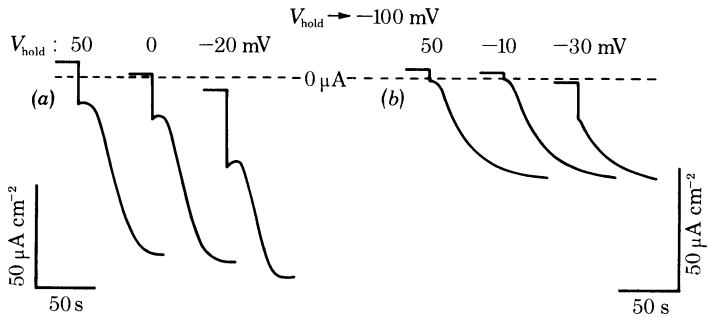

FIGURE 12. (*a*) Voltage-clamp currents of toad skin exposed to NaCl Ringer inside and KCl Ringer outside. If the holding potential (V_{hold}) is shifted towards negative values, the current activation at $V = -100$ mV is preceded by a positive-going current transient. (*b*) The type of current response depicted in (*a*) is not predicted by the model. The values of the input parameters used in these computations are listed in table 1, but the Na^+ of the outer compartment was replaced by K^+ to simulate the experimental conditions.

figure 11*a* is, in fact, similar to that seen in some experiments (see, for example, Larsen (1982) and figure 12*a*). However, if the Na^+ ions in the outer compartment are replaced by K^+ ions, the initial positive-going current transient is predicted to disappear (see figure 11*b*). This is in contrast to the toad skin in which the above response of clamping current depends on the presence of external Cl^-, but is independent of the cation composition of the external solution. This indicates that the initial positive-going current response is governed by a gating reaction, and not by accumulation–depletion processes.

Another piece of evidence for this interpretation comes from the current–time curves shown in figure 12. If the membrane is activated from a holding potential at which some channels are already open, the delay in current activation in the model disappears (figure 12*b*). This prediction does not stand when compared with the clamping currents in toad skin (figure 12*a*). As the holding potential is lowered, the response of the clamping current to a stepwise change of V to -100 mV shows an initial transient phase of a sign opposite to that expected from the new potential. Accordingly, it seems as though the rate coefficients of the gating reaction depend not only on the potential at which activation takes place, but also on the holding potential. In this respect, the kinetics of the Cl^- channels in toad skin resemble the kinetics of monazomycin or alamethicin channels in some artificial bilayers (Mueller 1975).

5. General discussion

(*a*) *Localization of the potential-dependent* Cl^- *conductance*

The results presented above provide good evidence that the potential plays a dual role for Cl^- transport in toad skin. Besides the classic view that the potential drives Cl^- through the

PHILOSOPHICAL TRANSACTIONS OF THE ROYAL SOCIETY B BIOLOGICAL SCIENCES

skin, it seems justified to conclude that the potential also controls the Cl^- permeability. Studies with frog skin have revealed a potential dependence of Cl^- transport of a nature similar to that of the toad skin (P. Kristensen, unpublished experiments). Furthermore, it has been shown that the unidirectional Cl^- fluxes through the short-circuited frog skin are depressed by reducing the Na^+ concentration of the outer bath (Kristensen 1978) or by blocking Na^+ transport by amiloride (Candia 1978; Kristensen 1978). These findings constitute strong evidence that Cl^- passes through cells that also take part in the transepithelial active Na^+ transport. A number of recent findings make it unlikely, however, that the transepithelial Cl^- flux passes through the granulosum cells, which, besides constituting the most abundant cell type of the epithelium, are responsible for the larger fraction of the transepithelial Na^+ transport.

In the first place, studies of the volume regulation of the granulosum cells of frog skin have identified two types of Cl^- transport system, however, both located in the latero-basal membrane (Ussing 1982*a*). These are (i) a co-transport system mediating a cellular uptake of Na^+ and Cl^- from the inner solution, and (ii) a passive Cl^- pathway. Ussing provides the evidence that the co-transport system normally operates with a low but sufficient rate to counteract the back-diffusion of Cl^- through a very low inner-membrane Cl^- permeability. The cellular Cl^- concentration is thereby maintained above its passive distribution, with small energy expenditure. This theory accounts for the finding that the Cl^- activity of the granulosum cells is significantly above its electrochemical equilibrium value (Nagel *et al.* 1981). If the cellular Cl^- concentration drops below a certain value, the co-transport system becomes activated. The Na^+ taken up by the co-transport system is returned to the inner bath in exchange with K^+ by the Na^+/K^+ pump, the net result being a cellular uptake of KCl. Cellular swelling seems to activate the passive permeability. Thus, by making the inner bathing solution hypotonic, cellular KCl is rapidly lost, but during recovery in normal Ringer solution, KCl is taken up again via the above mechanisms. These responses are independent of the composition of the solution bathing the external surface of the skin, indicating that the apical membrane of the granulosum cells is tight to Cl^-. Clearly, then, the Cl^- transport pathways of the granulosum cells serve to regulate cell water volume and intracellular Cl^- concentration, and not transepithelial Cl^- transport (Ussing 1982*a*, *b*).

Voûte & Meier (1978) found that the number of mitochondria-rich (m.r.) cells is linearly correlated with the passive Cl^- conductance in the frog skin, and they suggested that these cells are the site of the transepithelial shunt pathway. Kristensen (1981) showed that stimulation of active Na^+ transport by benzimidazolyl-guanidine (BIG) is associated with an increase of passive Cl^- flux in frog skin, whereas stimulation of Na^+ transport by antidiuretic hormone (ADH) leaves the passive Cl^- flux unaffected (in some skins a decrease was seen). Following his argument, this indicates that ADH increases Na^+ transport through cells that are not accessible to passive transepithelial Cl^- transfer. Because ADH stimulates the Na^+ transport through the granulosum cells (Nagel 1978; Dörge *et al.* 1981), it was concluded that the m.r. cells make up the cellular pathway for transepithelial Cl^- transport. Kristensen points out that this hypothesis is consistent with the hitherto puzzling observations that the Cl^- concentration of the granulosum cells is far above its electrochemical equilibrium value, yet a large dissipative Cl^- flux goes through a cellular compartment.

To account for all of the above findings, Kristensen & Ussing (1982) have proposed a revised model for frog skin, which includes both the granulosum cells and the mitochondria-rich cells as functional units for transepithelial ion transport (see also Ussing 1982*b*).

PHILOSOPHICAL TRANSACTIONS OF THE ROYAL SOCIETY B BIOLOGICAL SCIENCES

(*b*) *Relevance of the computer model analysis*

The theoretical approach used for the analysis of ion redistribution processes is based upon a three-compartment model, i.e. only a single cellular unit is considered. From the above discussion it is clear that this model is a greatly oversimplified description of the functional organization of the living tissue. However, we have reasons to believe that under certain experimental conditions it can give a useful insight into the effects of accumulation–depletion processes on voltage-clamp data. The significant points for the argument are that the potential-dependent Cl^- current passes only through the m.r. cells, and that these cells also take part in the amiloride-sensitive Na^+ transport, as was assumed for the model cell. The Na^+ and K^+ concentrations of the m.r. cells are similar to those of the granulosum cells, but within the individual skin preparations deviations between the cation concentrations of the m.r. cells and the granulosum cells could be observed (Rick *et al.* 1978). It was concluded that the mitocondria-rich cells are excluded from the syncytial unit formed by the other epithelial cells. The Cl^- concentration of the m.r. cells was not given, but as mentioned above it seems most likely that the value is governed by passive pathways. It can therefore be assumed that the mathematical model accounts for the electrical behaviour of preparations exposed to KCl Ringer outside, in which the granulosum cells do not seem to constitute any significant pathway for trans-epithelial current flow.

For $P^i_{Cl^-} \gg P^i_{K^+}$ and with KCl in the outer compartment, it is seen intuitively that ion redistribution currents are of little significance. The $P^i_{Cl^-}/P^i_{K^+}$ ratio of the m.r. cells is not known. In the computations we assumed that $P^i_{Cl^-} < P^i_{K^+}$, which is the case of interest for the theoretical analysis.

The choice of cell water volume of the model is important for the timescale of ion redistribution currents, but it is unimportant for the steady-state electrical behaviour. The epithelial cell water volume is about 4–5 μl cm^{-2} (Nielsen 1982). The volume of the m.r. cells is at most an order of magnitude less than this value (Whitear 1975), the important point being that the time constant of the ion redistribution currents is of the same order of magnitude as the gated currents. In the present study, therefore, we have analysed voltage-clamp data of the model for the likely case of approximately equal time constants of the two types of processes.

(*c*) *The apical membrane* Cl^- *permability*

With respect to the transport across the apical membrane, our study has posed two important questions. The first concerns the ion transport through open channels. The finding that the Cl^- conductance of the model does not saturate as the permeability becomes fully activated, as occurs in skin, provides evidence that the current–voltage curve of the open channels is linear in spite of an asymmetric distribution of Cl^- between the two sides of the membrane. In this respect, the Cl^- channels deviate from the Na^+ channels in frog skin, which for a fairly large voltage and concentration range exhibits current–voltage curves in agreement with the constant field theory (Fuchs *et al.* 1977). However, a detailed analysis is not possible unless the intracellular Cl^- concentration and the membrane potential can be monitored experimentally.

Another important observation is that the most simple kinetic scheme of the permeability activation fails to account for the voltage-clamp data under certain experimental conditions (figure 12). In the skin, the membrane conductance prevailing at the holding potential influences the kinetics of the current activation. This indicates that more than two configurations

PHILOSOPHICAL TRANSACTIONS OF THE ROYAL SOCIETY B BIOLOGICAL SCIENCES

of the Cl^- channels exist at a given moment. There is additional evidence that not just one but a series of membrane reactions control the Cl^- permeability. Thus inhibition of the cellular energy metabolism leads to a fast and reversible closure of the Cl^- channels (Larsen & Kristensen 1977), whereas application of theophylline increases the Cl^- permeability (Mandel 1975; Larsen & Kristensen 1977). Furthermore, it has been suggested that a decrease in the Cl^- concentration of the external solution reduces the Cl^- permeability (Kirschner 1970; Kristensen 1978; Ques-von Petery *et al.* 1978). The regulatory site has a high Cl^- specificity, in contrast to the Cl^- channels themselves, which do not discriminate strongly between Cl^-, Br^- and I^- (Kristensen 1982). Future studies may reveal whether phosphorylation processes or anion binding to the membrane have to be considered together with the potential gating in order to give a fuller account of the kinetics of voltage-clamp currents.

(*d*) *Possible implications of a potential-dependent* Cl^- *permeability*

Despite the fact that the kinetic scheme of the Cl^- permeability used in the above computations has been proved to be insufficient, we think that the hypothesis of a potential-controlled gate in the apical membrane Cl^- pathway is correct in its main outline. This finding provides a new way of thinking about the interdependence of Na^+ and Cl^- transport in tight epithelia. Because the outer membrane potential depends on the Na^+ current, it follows that activation of the Na^+ permeability also initiates a stimulation of the Cl^- permeability. However, further evaluation of the exact interdependence of the Na^+ current through the apical membrane and the Cl^- permeability must wait until the gating kinetics are more fully established.

We thank Professor H. H. Ussing for stimulating discussions. We also thank Mrs Lone Pedersen for assistance in the laboratory, and Mr Leif Andersen for writing programs for the computer on-line experiments. The study was supported by the Danish Natural Science Research Council, grant no. 11-0583 and by grants from the Novo Foundation.

References

Attwell, D., Eisner, D. & Cohen, I. 1979 Voltage clamp and tracer flux data: effects of a restricted extracellular space. *Q. Rev. Biophys.* **12**, 213–261.

Bruus, K., Kristensen, P. & Larsen, E. H. 1976 Pathways for chloride and sodium transport across toad skin. *Acta physiol. scand.* **97**, 21–47.

Candia, O. A. 1978 Reduction of chloride fluxes by amiloride across the short circuited frog skin. *Am. J. Physiol.* **234**, F437–F445.

Dörge, A., Rick, R., Katz, U. & Thurau, K. 1981 Determination of intracellular electrolyte concentration in amphibian epithelia with the use of electron microprobe analysis. In *Water transport across epithelia* (ed. H. H. Ussing, N. Bindslev, N. A. Lassen & O. Sten-Knudsen), pp. 36–51. Copenhagen: Munksgaard.

Frankenheuser, B. & Moore, L. E. 1963 The effect of temperature on sodium and potassium permeability changes in myelinated nerve fibres of *Xenopus laevis*. *J. Physiol., Lond.* **169**, 431–437.

Fuchs, W., Larsen, E. H. & Lindemann, B. 1977 Current–voltage curve of sodium channels and concentration dependence of sodium permeability in frog skin. *J. Physiol., Lond.* **367**, 137–166.

Helman, S. I. & Fisher, R. S. 1977 Microelectrode studies of the active Na transport pathway of frog skin. *J. gen. Physiol.* **69**, 571–604.

Helman, S. I., Nagel, W. & Fisher, R. S. 1979 Ouabain on active transepithelial sodium transport in frog skin. Studies with microelectrodes. *J. gen. Physiol.* **74**, 105–127.

Hodgkin, A. L. & Huxley, A. F. 1952 A quantitative description of membrane current and its application to conduction and excitation in nerve. *J. Physiol., Lond.* **117**, 500–544.

Hodgkin, A. L., Huxley, A. F. & Katz, B. 1952 Measurement of current–voltage relations in the membrane of the giant axon of *Loligo*. *J. Physiol., Lond.* **116**, 424–448.

Jørgensen, C. B., Levi, H. & Zerahn, K. 1954 On active uptake of sodium and chloride ions in anurans. *Acta physiol. scand.* **30**, 178–190.

PHILOSOPHICAL TRANSACTIONS OF THE ROYAL SOCIETY B BIOLOGICAL SCIENCES

Kirschner, L. B. 1970 The study of NaCl transport in aquatic animals. *Am. Zool.* **10**, 365–376.
Koefoed-Johnsen, V., Levi, H. & Ussing, H. H. 1952*a* The mode of passage of chloride ions through the isolated frog skin. *Acta physiol. scand.* **25**, 150–163.
Koefoed-Johnsen, V. & Ussing, H. H. 1958 The nature of the frog skin potential. *Acta physiol. scand.* **42**, 298–308.
Koefoed-Johnsen, V., Ussing, H. H. & Zerahn, K. 1952*b* The origin of the short-circuit current in the adrenaline stimulated frog skin. *Acta physiol. scand.* **27**, 38–48.
Kristensen, P. 1978 Effect of amiloride on chloride transport across amphibian epithelia. *J. Membrane Biol.* **40**, 167–185.
Kristensen, P. 1981 Is chloride transfer in frog skin localized to a special cell type? *Acta physiol. scand.* **113**, 123–124.
Kristensen, P. 1982 Chloride transport in frog skin. In *Chloride transport in biological membranes* (ed. J. A. Zadunaisky), pp. 319–332. New York: Academic Press.
Kristensen, P. & Larsen, E. H. 1978 Relation between chloride exchange diffusion and a conductive chloride pathway across the isolated skin of the toad (*Bufo bufo*). *Acta physiol. scand.* **102**, 22–34.
Kristensen, P. & Ussing, H. H. 1982 Epithelial organization. In *Physiology and pathology of electrolyte metabolism* (ed. D. W. Seldin & G. Giebisch). New York: Raven Press. (In the press.)
Larsen, E. H. 1982 Chloride current rectification in toad skin epithelium. In *Chloride transport in biological membranes* (ed. J. A. Zadunaisky), pp. 333–364. New York: Academic Press.
Larsen, E. H., Fuchs, W. & Lindemann, B. 1979 Dependence of Na-pump flux on intracellular Na-activity in frog skin epithelium (*R. esculenta*). *Eur. J. Physiol.* **382**, R13.
Larsen, E. H. & Kristensen, P. 1977 Effects of anoxia and of theophylline on transcellular Cl^--transport in toad skin. *Proc. Int. Union. Physiol. Sci.* **12**, 1002.
Larsen, E. H. & Kristensen, P. 1978 Properties of a conductive cellular chloride pathway in the skin of the toad (*Bufo bufo*). *Acta physiol. scand.* **102**, 1–21.
Larsen, E. H., Rasmussen, B. E. & Willumsen, N. 1981 Computer model of transporting epithelial cells. Analysis of current–voltage and current–time curves. In *Advances in Physiological Sciences* (ed. J. Salanki), vol. 3 (*Physiology of non-excitable cells*), pp. 115–127. Pergamon Press.
Lew, V. L., Ferreira, H. G. & Moura, T. 1979 The behaviour of transporting epithelial cells. I. Computer analysis of a basic model. *Proc. R. Soc. Lond.* B **206**, 53–83.
Lindemann, B. 1977*a* Circuit analysis of epithelial ion transport. I. Derivation of network equations. *Bioeletrochem. Bioenergetics* **4**, 275–286.
Lindemann, B. 1977*b* Circuit analysis of epithelial ion transport. II. Concentration- and voltage-dependent conductances and sample calculations. *Bioelectrochem. Bioenergetics* **4**, 287–297.
Mandel, L. O. 1975 Actions of external hypertonic urea, ADH, and theophylline on transcellular and extracellular solute permeabilities in frog skin. *J. gen. Physiol.* **55**, 599–615.
Moore, J. W. 1958 Temperature and drug effects on squid axon membrane ion conductance. *Fedn Proc. Fedn Am. Socs exp. Biol.* **17**, 113.
Mueller, P. 1975 Membrane excitation through voltage induced aggregation of channel precursors. *Ann. N.Y. Acad. Sci.* **264**, 247–264.
Nagel, W. 1976 The intracellular electrical potential profile of the frog skin epithelium *Pflügers Arch. Eur. J. Physiol.* **365**, 135–143.
Nagel, W. 1977 The dependence of the electrical potentials across the membranes of the frog skin upon the concentration of sodium in the mucosal solution. *J. Physiol., Lond.* **269**, 777–796.
Nagel, W. 1978 Effects of antidiuretic hormone upon electrical potential and resistance of apical and basolateral membranes of frog skin. *J. Membrane Biol.* **42**, 99–122.
Nagel, W. & Crabbé, J. 1980 Mechanism of action of aldosterone of active sodium transport across toad skin. *Pflügers Arch. Eur. J. Physiol.* **385**, 181–187.
Nagel, W. Garcia-Diaz, J. F. & Armstrong, W. McD. 1981 Intracellular ionic activities in frog skin. *J. Membrane Biol.* **61**, 127–134.
Nielsen, R. 1982 Effect of ouabain, amiloride, and antidiuretic hormone on the sodium-transport pool in isolated epithelia from frog skin (*Rana temporaria*). *J. Membrane Biol.* **65**, 221–226.
Ques-von Petery, M. V., Rotunno, C. A. & Cereijido, M. 1978 Studies on chloride permeability of the skin of *Leptodactylus ocellatus*. I. Na^+ and Cl^- effect on passive movements of Cl^-. *J. Membrane Biol.* **42**, 317–330.
Rick, R., Dörge, A., Arnim, E. von & Thurau, K. 1978 Electron microprobe analysis of frog skin epithelium: evidence for a syncytial sodium transport compartment. *J. Membrane Biol.* **39**, 313–331.
Sten-Knudsen, O. 1978 Passive transport processes. In *Membrane transport in biology* (ed. G. Giebisch, D. C. Tosteson & H. H. Ussing), vol. 1 (*Concepts and models*), pp. 5–113. Berlin, Heidelberg and New York: Springer-Verlag.
Tsien, R. W. & Noble, D. 1969 A transition state theory approach to the kinetics of conductance changes in excitable membranes. *J. Membrane Biol.* **1**, 248–273.
Ussing, H. H. 1949 The distinction by means of tracers between active transport and diffusion. *Acta physiol. scand.* **19**, 43–56.

PHILOSOPHICAL TRANSACTIONS OF THE ROYAL SOCIETY B BIOLOGICAL SCIENCES

Ussing, H. H. 1978 Interpretation of tracer fluxes. In *Membrane transport in biology* (ed. G. Giebisch, D. C. Tosteson & H. H. Ussing), vol. 1 (*Concepts and models*), pp. 116–140. Berlin, Heidelberg and New York: Springer-Verlag.

Ussing, H. H. 1982*a* Volume regulation of frog skin epithelium. *Acta physiol. scand.* **114**, 363–369.

Ussing, H. H. 1982*b* Pathways for transport in epithelia. In *Functional regulation at the cellular and molecular levels* (ed. R. A. Corradino), pp. 285–297. Amsterdam: Elsevier/North-Holland.

Ussing, H. H. & Windhager, E. E. 1964 Nature of shunt path and active sodium transport path through frog skin epithelium. *Acta physiol. scand.* **61**, 484–503.

Ussing, H. H. & Zerahn, K. 1951 Active transport of sodium as the source of electric current in the short-circuited isolated frog skin. *Acta physiol. scand.* **23**, 109–127.

Voûte, C. L. & Meier, W. 1978 The mitochondria-rich cell of frog skin as hormone sensitive 'shunt path'. *J. Membrane Biol.* **40**, 141–165.

Whitear, M. 1975 Flask cells and epidermal dynamics in frog skin. *J. Zool., Lond.* **175**, 107–149.

Willumsen, N. & Larsen, E. H. 1981 Time- and voltage-characteristics of a passive Cl^- pathway in the isolated skin of *Bufo bufo*. *Acta physiol. scand.*, Abstract Book from the Scandinavian Physiological Society Meeting in Århus, p. 28A.

Zadunaisky, J. A., Candia, O. A. & Chiarandini, D. J. 1963 The origin of the short-circuit current in the isolated skin of the South American frog *Leptodactylus ocellatus*. *J. gen. Physiol.* **47**, 393–402.

PHILOSOPHICAL TRANSACTIONS OF THE ROYAL SOCIETY B BIOLOGICAL SCIENCES